FROM BUTTERFLY TO PROPELLER

Igor S. Kovalev *[1]
[1]Science and Technology Laboratory, Kinneret College, Emek Hayarden, 15132, Israel

Résumé

Le potentiel de la "peau acoustique du papillon", en tant que nouvelle méthode de réduction du bruit aéroacoustique pour une hélice silencieuse, a été évalué. Ce sujet est particulièrement pertinent en raison de l'augmentation des hélices à usage civil comme militaire avec de multiples problèmes opérationnels. La réduction du bruit comme l'efficacité d'un système propulsif sont des aspects clés dans la conception des véhicules aériens avancés et peuvent très souvent conduire au succès ou à l'échec d'une mission. L'attention a été portée sur ce problème par l'observation des écailles poreuses de lépidoptères et de leurs propriétés de réduction du bruit : la couverture des mites permet à ces insectes de surmonter les attaques des chauves-souris la nuit. Ces appendices sont très petits (taille : 30 - 200 µm) et ont une structure poreuse différente. Bien que de nombreuses structures d'écailles poreuses de lépidoptères aient été discutées, seules les écailles poreuses des papillons *Papilio nireus* et *Delias nigrina* sont abordées ici. Deux conceptions de "peau acoustique de papillon" imitent les écailles creuses des ailes du papillon *Papilio nireus* (région creuse) et du papillon *Delieas nigrina* (région poreuse). Les résultats illustrent l'influence de structure de type "peau acoustique du papillon" sur les performances acoustiques d'une hélice à deux pales. Pour un nombre de Reynolds de 200000, la réduction du bruit d'une hélice en rotation type "peau acoustique de papillon" à région poreuse est de 4 dB, quand une hélice de type "peau acoustique de papillon" à région creuse est de 2 dB. La modification des effets acoustiques sur l'hélice en rotation avec la "peau acoustique de papillon" est due à la fois à une absorption acoustique, à une dissipation de l'énergie turbulente, à une réduction de l'influence sur le bruit généré et à une réduction de la différence de pression. D'autres études sur la "peau de papillon" ont montré que cette structure augmentait la force de portance et réduisait les vibrations de l'aile. Une étude expérimentale de l'effet du BAS sur les vibrations et les performances aérodynamiques de l'hélice n'entrait pas dans le cadre de cette expérience. Une explication complète, avec différentes vitesses de vent et de rotation des pales, est attendue pour des études plus détaillées. Mais il ne semble pas déraisonnable de suggérer la possibilité d'une géométrie optimale du BAS et de sa structure pour augmenter encore la poussée et réduire le bruit et les vibrations de l'hélice.

Mots clefs : *lepidopterans*, bruit, écailles poreuse, hélices, peau.

Abstract

The potential of the 'butterfly acoustical skin', as a new method of reduction aero acoustical noise for a quiet propeller, has been evaluated. This topic is particularly relevant due to the increase of the propellers for civil and military purposes with multiple operational issues. The quietness and efficiency of the propulsive system are key aspects in the design of advanced aerial vehicles and very often can lead to the success or failure of a mission. Attention was directed to this problem by the observation of the porous scales of *lepidopterans* and of there noise reduction properties: the moth coverage allows these insects to overcome bat's attacks at night. These appendages are very small (size: 30 – 200 µm) and have a various porous structure. Althought many structures of the porous scales of *lepidonterans* were discussed, here only the porous scales of the butterflies *Papilio nireus* and *Delias nigrina* are discussed. Two designs of "acoustic butterfly skin" imitate the hollow scales on the wings of the *Papilio nireus* butterfly (hollow region) and the *Delieas nigrina* butterfly (porous region). The results illustrate the influence of "acoustic butterfly skin" type structure on the acoustic performance of a two-bladed propeller. For a Reynolds number of 200,000, the noise reduction of a rotating propeller of the "acoustic butterfly skin" type with a porous region is 4 dB, when a propeller of the "acoustic butterfly skin" type with a hollow region is 2 dB. The modification of acoustical effects on the rotating propeller with 'butterfly acoustical skin' was due both to an acoustic absorption, to a dissipation of turbulent energy, to a reducing influence on noise generated and to reducing the pressure difference. It was determined in qualitative researches that the 'butterfly acoustical skin' influenced on the acoustic perfor-mances of two-bladed propeller. Other studies of 'butterfly skin' shoved that the skin increased the lift force and reduced the wing vibration. An experimental investigation of the effect of BAS on vibration and aerodynamic performances of propeller was not within the scope of this experiment. A full explanation, with different wind speeds and blade RPM, must await more detailed studies. But it does not seem unreasonable to suggest the possibility of some optimal BAS geometry and its structure to further augment thrust and reduce the noise and vibration of propeller.

Keywords: *lepidopterans*, noise, porous scales, propeller, skin.

1 Introduction

1.1 Propeller

A propeller is a type of aeronautical propulsion system that transmits power by converting rotational motion into thrust. A history of aerodynamic propeller usually begins with mention of the Chinese flying top (ca. 400 B.C.) which was a stick with a propeller on top, which was spun by hands and released [1]. Among da Vinci's works (late 15th century) there were sketches of a machine for vertical flight using a screw-type propeller. The Wright brothers designed and tested aerodynamic propellers, and made the first powered flight in 1903 (Figure 1. a). Propellers were the first means of powering airplanes, preceding all other means of propulsion by about 40 years. This aeronautical propulsion system was used extensively through 1940's.

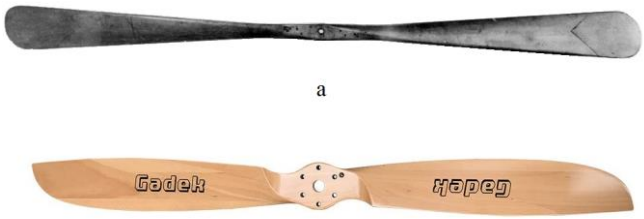

a

b

Figure 1: Wright brothers' propeller, b. Gadek propeller (2019).

Although there have been many refinements to propellers through the years, the general appearance of the propellers has changed little (Figure 1). An aircraft propeller can be described as an open, rotating and bladed device [2]. Today, a renewed attention is being focused on the first aeronautical propulsion device - the propeller. This is due to the increased use of unmanned aerial vehicles [3], the growing market of general aviation, the increasing interest in ultra-light categories or light sport air vehicles, and the growing importance of environmental issues that have led to the development of all-electric emissionless aircrafts [4].

One of the most disturbing problems of propeller-driven aircraft was and still is their noise, which may limit the aircraft's operation. On the whole, the frequency range for human hearing, commonly referred to as audio frequencies, is typically cited as approximately 20 Hz – 20 kHz [4]. And while the human ear is sensitive to sounds between 0 and 140 dB, the sound level (140 dB) is too painful to the listener [5]. In propeller-based propulsion systems, the main sources of noise are the engine and the propeller. Propeller aircraft noise reduction has been studied since the early days of aviation. Initially the need for noise reduction was coupled with the need for reduced detectability in military operations [6]. Noise generated by aircrafts can propagate into the airport neighborhood and into the aircraft interior causing annoyance and discomfort of residents and passengers [7]. For example: the noise generated from the propeller of the aircraft XF 84 H was 135 dB and reportedly heard as far away as 40 km. This aircraft was not very popular with pilots. The propeller – driven strategic bomber Tu – 95 is considered to be the noisiest flying machine in current world aircraft. US submarines can detect the aircraft flying high overhead through their sonar domes while still underwater.

The acoustic signature of military aircraft has a signifycant effect on their detection. The importance of noise signature of propeller-driven air vehicles was already noticed during the 1960s [8]. Today, with the increased use of propeller-driven vehicles, there is a renewed interest in reducing the noise of propellers [9]. Many airports around the world impose strict limitations on noise level permitted during day or night.

One of the most commonly known methods of reducing aero acoustic noise is a blade geometry modification. It is well known, that different parameters in details among various designs, such as number of blades, blade shape, propeller diameter, blade pitch, trailing edge geometrical modifications and propeller blade fineness have impact on acoustic noise [10]. The propeller noise can be reduced by increasing blade sweep, reduction of blade thickness and reduction of tip speed [2].

1.2 Porous wing scale of *lepidopterans*

Bio mimicry, sometimes called bionics, is the application of biological processes and forms found in nature to the study design of engineering systems [11]. Butterflies and moths both belong to the insect order *Lepidoptera*. These insects are usually called *lepidopterans* [12]. The surface of the wings of the *lepidopterans* is covered with millions of tiny movable appendages – scales (30-200 μm in size) [13] (Figure 2. a, c). In contrast to the butterflies, all body parts (a head, a thorax and an abdomen) of the moths are covered with abundant appendages (scales and micro bristles) (Figure 2. c, d). It is well known that the *lepidopterans* scale coverage reduces the potential of the reflected ultrasound signal from a flying moth [14 - 17], minimizes the noise [18] and the vibration in flying insects [19]. When an ultrasound wave strikes the *lepidopterans* surface, so significantly part of bat's calls and noise of a flying insect are transformed into heat in the pores of the scale coverage [14, 16, 17]. This way, the property of the coverage allows the insect to overcome predator's attack at night. These facts motivated the work presented in this paper.

The micro – and nanostructure of the *lepidopterans* wing scales is a true miracle of nature. Each scale of the butterfly *Papilio nireus* resembles dorsoventrally flattened sacs with an upper UL (also called obverse) and lower LL (also called reverse) lamina (Figure 2. b). The region between the upper UL and the lower LL lamina is termed the lumen Lu. The structure of the reverse lamina is generally undifferentiated. Both surfaces of this lamina are smooth, whereas the obverse lamina (Figure 2. b) possesses an intricate architecture, typically is composed of a series of longitudinal ridges Lr and of a porous structure (PS). The porous structure of UL has porosity values over 60 – 70 percent; the pore diameter is 240 nm, the scale thickness (without ridges Lr) is 3 m [20].

The upper lamina of the porous scales of the butterfly *Delias nigrina* (Figure 2. c and d) is a complex structure. This

* kovis@ashdot-m.org.il

lamina composed of a series of longitudinal ridges and a series of cross ridges (CR). Longitudinal ridges and cross ribs frame open pores to the scale interior. The obverse lamina (Figure 2. d) has porosities from 40 to 50 per cent; the average size of the open pores is 1×1 µm. The lumen Lu of the porous appendages are abundantly studded with micro beads (MB) (Figure 2. d [22]). This type of porous structure has been classified as 'pigment granules' [22]. Every micro bead is elongated micro ovoid with dimensions of 100-500 nm [22]. This porous structure has porosity values over 30-40 percent, the scale thickness (without ridges Lr) is 1.5 µm.

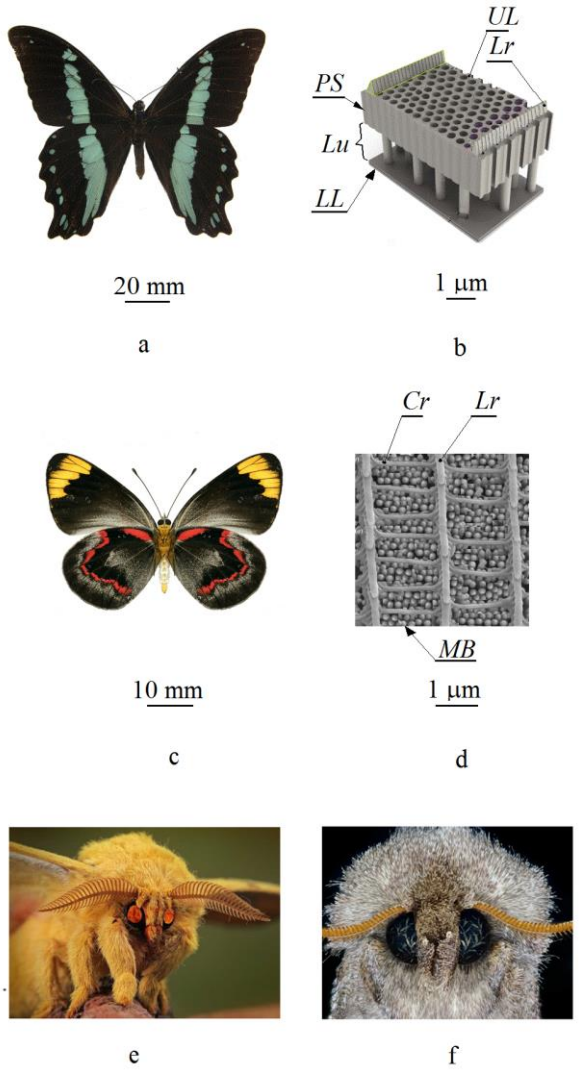

CR - cross ridges; LL - lower (reverse) lamina; Lr - longitudinal ridges; UL – upper (obverse) lamina; Lu – lumen; MB - micro beads; PS - porous structure.

Figure 2: a. Dorsal wing surfaces of butterfly *Papilio nireus*. b. Nanostructure (vertical cross-section) of a cover porous scale of *Papilio nireus*, drawn in 30 ° isometric [20, 21]. c. Dorsal wing surfaces of butterfly *Delias nigrina*. d. SEM showing a plane view of cover porous scale of *Delias nigrina*. The scales are studded with pigment granules MB [22]. e. A moth of *Saturniidae* family, f. A front view of a moth's head (*Noctuoidea* family).

2 Material and experimental methods

2.1 Wind-tunnel

The aero acoustic features of low-speed propellers were tested in the Zaporozhe Machine-Building Design Bureau (ZMBDB) low speed straight through a wind-tunnel (Figure 3). Air was driven from a high pressure storage HPS through the valve Va into a wide chamber WC with a low velocity. A screen S of wire gauze helped to equalize the velocity, across the cross-section of the chamber. A honeycomb H ensured that there was no large-scale swirling around in the channel, and that the air traveled along it in straight lines. The irregularity of wind of the wide chamber was swamped by the large space. Thus a uniform increase in velocity that occurred when the air passed through the narrower nozzle N (diameter of 2000 mm) was attained. A contraction section of the nozzle was designed using a matched pair of cubic curves. Thus, the airstream in the working section was uniform (the drift of the free stream velocity was less than about 0.9 %) and laminar (the free stream turbulence level was less than 0.5 % of the free stream velocity). The air speed of the wind tunnel was 30 m/s. One typical Reynolds based on chord length on this wind speed was 200000.

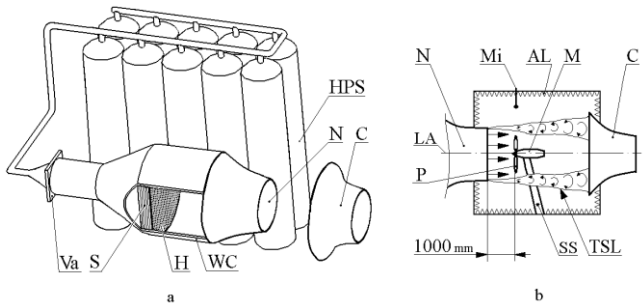

AL – Acoustic lining; P – propeller; Mi –microphone; M – motor; C – collector; H - honeycomb flow straightened; HPS - high pressure storage; N - nozzle; S – screen; Va – valve; WC - wide chamber; TSL - turbulent shear layer; SS - supporting strut; LA - longitudinal axis of the wind-tunnel.

Figure 3: a. Axonometric view of the ZMBDB wind tunnel, b. Transverse view (along the longitudinal axis LA) of experimental apparatus installed in the ZMBDB wind tunnel open test section.

Test section winds were measured using a Pitot-static tube connected to a Datametric Barocel Electronic Manometer. Pressure differences down to 0.0001 in H2O could then be measured. Turbulent velocity data and mean speed were also measured by using a constant temperature hot-wire anemometer. Air temperature was maintained at 20 ˚C.

All aero acoustic tests were carried out on two bladed propellers in the square anechoic room (length was 6 m, width was 4 m, and the height was 3 m) lined with absorptive acoustic wedges. Room location was at the Research Center of ZMBDB. The energy cut-off of the anechoic wedges had a sound absorption coefficient at normal incidence greater

than 0.99. The collector was downstream of the test section. Noise-absorbing furry materials were attached to the surface of the collector to reduce the interaction noise between the open jet and the collector. The background noise was about 34 dB at a free stream velocity of 30.0 m/s. Figure 3 shows a picture of the chamber and a sketch of the layout of the experimental setup.

The measurements of noise were made during the evolution of the low-speed propellers in the square anechoic room. The acoustic instruments were produced by Brüel & Kjær and consisted in a sound and vibration analyzer Pulse-X3570 integrated with FFT and CPB analysis tools, a Nexus 2690 amplifier and 1 free field ¼" microphones type 4939 with a dynamic range of 28 Hz to 164 kHz, 200 V polarization. The sensitivity calibrated at 250 Hz by using piston phone type 4228 with ¼" adaptor DP 0775. The narrowband sound pressure level spectra were computed with a Fast Fourier Transform size of 8192, giving a frequency resolution of 0.2 Hz. The sampling frequency of acoustic instruments spans from 0.026 Hz to 28 Hz, depending on the maximum frequency to measure, and on the number of lines of discretization. In these measurements the author has adopted a resolution in the range 0.026 – 0.25 Hz, which guarantees a quite sharp definition of the acoustic discrete tones. The temperature and humidity inside the anechoic room were recorded to enable computation of the atmospheric absorption. The sound pressure levels (SPL) spectra were corrected for actuator response free-field correction, and atmospheric absorption. The overall sound pressure level (OSPL) was calculated through integration of SPL spectrum.

Previous theoretical predictions [23, 24] and experimental researches [25] showed that, when the observer/ microphone moved from the axial location toward the rotation plane, the harmonic contribution of propeller noise became more evident, while the broadband term decreased, and then eventually the harmonic contribution dominated over the other contributions in proximity of the rotational plane. Following these conclusions, the microphone was attached to the anechoic room ceiling and lay in the intersection of two planes: the rotation plane and the vertical plane along the longitudinal axis of the wind-tunnel. The sensor was placed out of the air stream one diameter from the center of the propeller rotation, and the microphone locations were outside of the turbulent shear layer TSL. The position of the microphone relative to the propeller is shown in Figure 3.

The propellers were driven by an electro motor M, which provided a power of 102 kW at a rotational speed of 1780 rpm (revolutions per minute). The motor pylon was mounted to an aerodynamically shaped strut SS which was securely anchored to the floor by means of steel tracks embedded into it (the floor and the supporting strut were then covered with acoustic foams). Power was supplied by a 240 V three-phase electrical bus and controlled from the observation room. This allowed the experimenter to operate both the data acquisition software and experimental apparatus from one location set in an adjacent room where a designated control desk was set. The motor controller of choice was selected due to its external display (indicating motor rotational speed) and compatibility with an external potentiometer used to finely adjusts the motor's revolutions per minute. In order to mount the propellers on the shaft of the motor, an aluminum adapter was produced, to ensure that the ambient noise, which also includes the noise from the electrical motor itself, is not excessively high. The total sound pressure level of the motor was 39 dB at a free stream velocity of 30.0 m/s. A set of measurements was taken with the free electrical motor alone, and it was found that for rotational speeds exceeding 1780 rpm the background noise was small.

2.2 Propellers

Three different propellers were used (Figure 4. a, b and c). The skin of first propeller (Figure 4. a) imitated the cover hollow wing scale of the *Papilio nireus* butterfly (Figure 2. b). This skin called Smooth Butterfly Skin with a Hollow Region (SBSwHR) (Figure 4. a) was 400 times life size (the thickness was 1.2 mm) (Figure 4. a, b). SBSwHR was composed of two layers. The upper metal wall UW (the thickness was 0.5 mm) and the lower metal wall LW (the thickness was 0.2 mm) were separated by an air cavity AC (0.5 mm in clear spacing) Figure 4. d). Both metal layers were joined by vertical supports VS. The facing surface and opposite side of the UW were smooth. The external wall (UW) provided with diagonally staggered rows of round perforation (hole diameter was 0.5 mm). The porosity of the UW was 40 %. This metal wall was manufactured by ANDRITZ Fiedler Company. The lower metal wall LW was similar to a thin sheet. Since, the propeller blade shape was very complex and different, the blade was made with eleven butterfly skin segments. The butterfly skin segments were formed around the blade. Initially, every segment was supported by the propeller body and was affixed on the smooth outer surface of the propeller blade. Then, the segments were disposed very close to each other. Finally, every abutment joint was covered with glue putty and was formed a flush joint.

The skin of the second propeller imitated the cover porous wing scale of the *Pieris rapae* butterfly and the cover porous wing scale of the *Delias nigrina* butterfly (Figure 2. c). This skin called Smooth Butterfly Skin with a Porous Region (SBSwPR) (Figure 4. b) was 800 times life size (the thickness was 1.2 mm) (Figure 4). SBSwPR was composed of free layers (Figure 4). The experimental studies by Pechan and Sencu [26] and by Hamacawa et al. [27] showed that various surface imperfections (groove, ridge, et cetera) of the propeller blade [26] or of the airfoil [27] may generate the noise. So, the faicing surface and opposite side of UW were smooth. The upper metal wall UW of the SBSwPR was geometrically similar to the UW of the SBSwHR. The lower metal wall LW was similar to a thin sheet. The air hole between UW and LW and the round hole perforations of the UW were filled with porosity material. The sintered powder stuffing SPS was manufactured by ZMBDB. The thickness of the UW was 0.5 mm, the thickness of the SPS was 0.5 mm and thickness of the LW was 0.2 mm. The aluminum powder AP sizes were in the range of 50 μm to 65 μm, and inter particle porosity IP was 35 % (Figure 4. f). The facing

surface of the UW was disposed flush the exterior surface of the powder stuffing (Figure 4. l). The sintered production process is described in detail in work [28]. A brief description of this process is submitted follows.

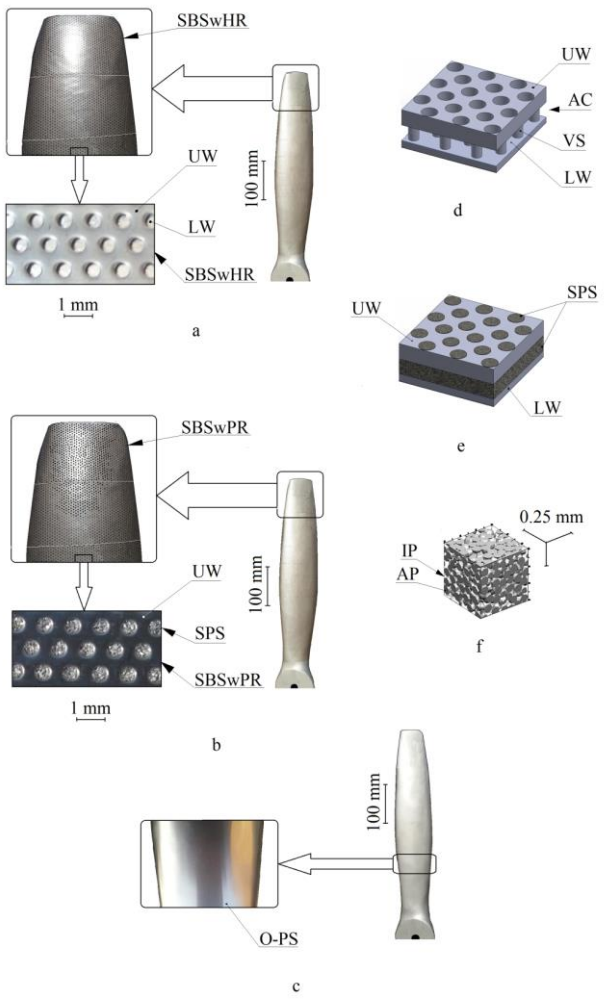

SBSwHR: UW - upper metal wall; AC - air cavity;
VS - vertical support; LW - lower metal wall;
SPS - sintered powder stuffing;
SBSwPR: smooth butterfly skin with a porous region;
AP - aluminum powder; IP - inter particle porosity;
O-PS - one-piece skin.

Figure 4: Front view of three propellers. a. propeller with SBSwHR, b. propeller with SBSwPR, c. propeller with one-piece skin, d. a vertical cross-section of the smooth butterfly skin with a hollow region in axonometric plane, e. a vertical cross-section of the smooth butterfly skin with a porous region in axonometric plane, f. 3D computer tomography of the sintered powder stuffing in axonometric plane.

Initially a hydraulic press, cold-molding die was made. Then, an aluminum powder with an incorporated amount phenolic binder was poured into the die. Next, the die assembly was jogged to settle the powder, and baked at 230 °C to cure the phenolic binder. Finally, the stuffing was removed from the die in the molded-and-cured form ready for sintering. The stuffing was sintered at 560 °C for four hours in vacuum of 1×10^{-6} to 1×10^{-7} Torr. This sintered process used the alumi-num powders, which were manufactured by Valimet Inc. Similar to the first propeller which the SBSwHS, the blade of second propeller was made with eleven segments of the SBSwPR (Figure 4. b). Similarity these butterfly skin seg-ments were formed around the blade, and as well each seg-ment affixed on the smooth outer surface of the second propeller blade, and were disposed very close to each other, and formed a putty flush joint. For the structural design of the SBSwPR there are not equivalents in the modern porous media.

Since the SBSwHR and the SBSwPR imitated the cover wing scales of one order – *Lepidoptera*, so the author incur-porated both these skins (SBSwHR and SBSwPR) into one group – 'butterfly acoustical skin' - BAS.

It is the principal concern of this study to qualitatively determine the effect of butterfly skin on the rotating propeller acoustic. Therefore, the metal skin (O-PS) of the third propeller was one-piece, smooth and airproof. The skin thickness was 1.2 mm. The blades of the third propeller were hand-finished (Figure 4. c) to highly smooth and polished surfaces, using 12000 - grit sand paper. The skin was chaped around the blade, and was affixed on the smooth outer surface of the third propeller blade. All the three propellers had identical geometric parameters: airfoil sections (NACA 2415), diameter (1200 mm), thickness, chord and pitch. The acoustical properties of the third propeller were compared with that of the first and second propellers.

3 Results

This section presents the acoustic results for the three propellers. The discussion focuses on the blade passing frequency (BPF) tones of these propellers. Figure 5. a, b and c corresponding to the blade skin displayed in Figure 5 for rotational speed 1780 rpm. The frequency along the horizon-tal axis ranges from 0 to 3,800 Hz, covering both the narrow-band and the broadband parts of the total noise. The harmonic part is shown in the lower frequency range (e. g. from 0 to ~3,250 Hz for smooth skin in Figure 5. a, and from 0 to ~2,200 Hz for hollow skin in Figure 5. b). The tonal noise levels represent most of the contribution to the total noise (Figure 5. a and b), while the broadband noise represents only a small portion.

Initially, the author examined the smooth rotating propeller acoustics. Figure 5. a displays the near field narrow-band SPS spectra in the rotor plane. In this plane the fundamental BPF ton 1 and its higher harmonics up to tone 6 is dominant. The peak of the tone 1 is 25 dB above the broadband noise. Figure 5. a shows that rotating propeller generated tones at harmonics of 567 Hz at high levels over 65 dB extending from low frequencies to approximately 2,700 Hz. These rotating propeller tones begin at 82.6 dB and drop to approximately 63 dB at 3,250 Hz. The total sound pressure level OSPL of the rotating propeller with the smooth skin, which takes into account the entire frequency domain (0…100 kHz), is 56.5 dB.

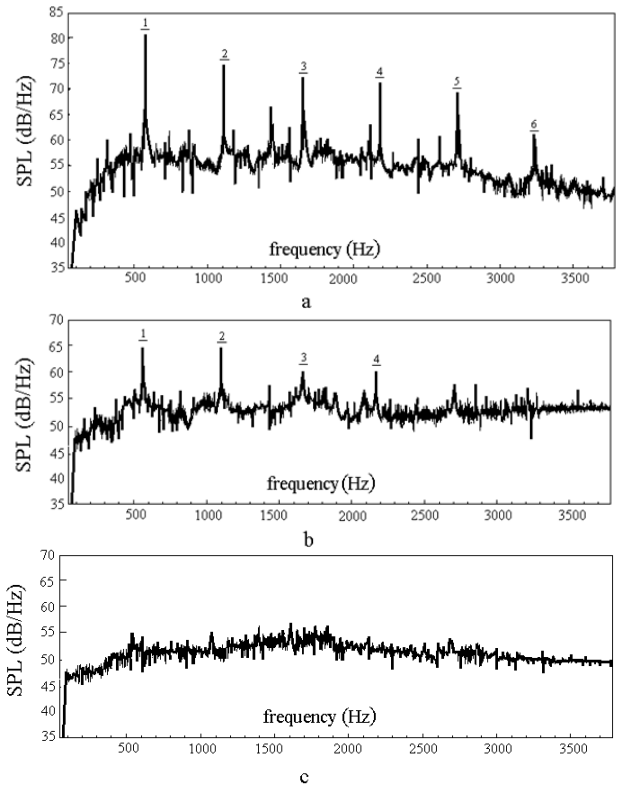

Figure 5: Near field SPL spectra for the rotating propeller with smooth skin (a), hollow skin (b) and porous hollow skin (c).

Then, the author examines the impact of the hollow skin on rotating propeller acoustics. Figure 5. b plots the near field noise narrow band and broadband SPL spectra from rotating propeller with the hollow skin in the rotor plane. Multiple peaks are observed on the spectrum. Examining the spectrum the author clearly distinguishes tones 1, 2, 3 and 4. The author observes a temperate content of tones, with the principal ones labeled. The fundamental BPF tones 1 and 2 are dominant and have similar magnitude. The next stronger tones 3 and 4 are about 3 dB lower than the dominant tones. Higher harmonics 5 and 6 are buried in the broadband noise. The maximum peak level of the spectrum is approximately 18.6 dB lower than the higher harmonic 1 of the propeller with the smooth skin at 567 Hz. Therefore, this skin is effective to reduce the tonal noise from the rotating propeller. On the other hand, the broadband noise is slightly increased from 2,300 Hz to 3,800 Hz for the rotating propeller with hollow skin (Figure 5. b). One of the main mechanisms of generating higher amplitude broadband noise is the turbulent boundary layer flow developing over the porous outer surface of the hollow skin. The skin increases the velocity disturbance in the boundary layer on the porous outer surface of the rotating propeller, and increases the turbulent noise [29]. The total sound pressure level OSPL of the rotating propeller with the hollow skin, is 54.2 dB. A quantitative comparison of the sound pressure levels shows that the total sound level of the rotating propeller with the hollow skin is more than 2 dB lower with respect to the one with the smooth skin. This result compares well with the noise reduction of a stator vane by passive porosity [30].

Finally, the author examines the impact of the porous hollow skin on the rotating propeller acoustics. Figure 5. c displays the near field noise from rotating propeller with the porous hollow skin in the rotor plane. No peaks are formed in the spectra – all harmonics are buried in the broadband noise. The broadband part dominates over the other contributions in the rotor plane. Based on the spectra results (Figure 5. c), it seems that the most effective mechanism of reducing the acoustic waves in the harmonic part of the noise spectrum is the rotating propeller with the porous hollow skin. Moreover, Figure 5. c shows a slight decrease in the broad band noise level from 2,300 Hz to 3,800 Hz for the propeller. It is clear that the porous hollow skin is more efficient in reducing broadband noise than the hollow skin. This suggests that the porous diameter of the porous hollow skin (0.1 mm) is less efficient in exciting the turbulent noise than the one of the hollow skin (0.5 mm). The total sound pressure level OSPL of the rotating propeller with the porous hollow skin, is 52.5 dB. A quantitative comparison of the sound pressure levels shows that the total sound pressure level of the rotating propeller with the porous hollow skin is more than 1.5 dB lower with respect to the one with the hollow skin and is more than 4 dB lower with respect to the one with the smooth skin. The latter result compares well with the noise reduction of the porous-bladed fan given by Chanaud at al [31].

4 Discussion

4.1 Propeller noise reduction

The major propeller noise components are thickness noise (due to the volume displacement of the blades), steady-loading noise (due to the steady forces on the blades), unsteady-loading noise (due to circumferentially nonuniform loading), quadrupole (nonlinear) noise, and broadband noise [32]. Each one of these components acts on the blade surfaces.

Noise absorption mechanism of propeller with SBSwPR

Sarradj E. and Geyer [29] showed the noise reduction mechanism by porous airfoils. The author developed the mechanism of propeller noise reduction by SBSwPR on the basis of Sarradj's and Geyer's mechanism. Noise absorption of a propeller with SBSwPR follows three aspects. The first of these aspects is acoustic absorption. Sintered powder stuffing of SBSwPR contains through pores and micro channels so that sound waves are able to easly enter through them. When sound enters the stuffing, owing to sound pressure, air molecules oscillate in the interconnecting voids that separate the micro granules with the frequency of the exiting sound wave. This oscillation results in frictional losses. A change in the flow direction of sound waves, together with the expansion and contraction phenomenon of flow through irregular pores, results in a loss of momentum. Owing to the exciting of sound, air molecules in the pores undergo periodic compression and relaxation. This results in change of temperature. Because of long time, large surface to volume ratios and high heat conductivity of powder stuffing, heat exchange takes place isothermally at low frequencies. At the same time in the high frequency region compression takes

place adiabatically. In the frequency region between these isothermal and adiabatic compression, the heat exchange results in loss of sound energy. So, the reasons for the acoustic energy loss when sound passes through sound absorbing materials are due to: frictional losses, momentum losses and temperature fluctuations [33, 34]. Another possible aspect is the dissipation of turbulent energy from boundary layer by the porous surface. This would also result in less broadband noise generation at the trailing edge. The third aspect is the reducing influence on noise generated by the contact of turbulence with leading edge and also on other noise generation components. In addition, scattering of the micro granules also influences the absorption of sound energy inside the powder stuffing

Propeller noise reduction mechanism by SBSwHR

It is well known, that fan noise reduction can be achieved either by design aiming for it at the source or by incorporating acoustic treatment to absorb the noise produced by the source [35]. Approaches to reduce noise at the source are based on the fact that any of the significant noise generating mechanisms is related to unsteady, periodic forces acting on the surfaces of rotating fan, and caused by gust-type disturbances. These unsteady forces give rise to acoustic perturbations that propagate through the fan duct and radiate as noise. The noise level generated from this source is directly proportional to the magnitude of the fluctuating lift force. Thus, any reduction in this fluctuating force would result in a reduction in noise.

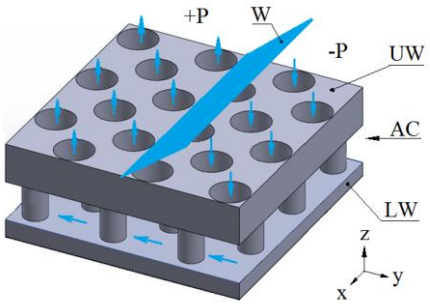

AC – air cavity; W – sound wave; UW – upper wall;
LW – lower wall; +P – high pressure region;
-P – low pressure region

Figure 6: The influence of the sound wave W on the SBSwHR, drawn in axonometric.

Tinetty A.F. et al. [35] shows the mechanism to reduce interaction noise in turbo machinery by passive porosity on the stator vane. The author developed the mechanism of a propeller noise reduction by SBSwHR on the basis of Tinetty's mechanism. Figure 6 shows a schematical drawing of what may be assumed to happen. In Figure 6 plotted a local sound wave W in (Y-Z-X) plane around a fragment of SBSwHR in an axonometric view. A rotating propeller produces unsteady and periodic forces acting on the porous outer surface of SBSwHR, which result in sound wave radiation. The sound wave produces the high-pressure region +P and the low-pressure region –P on the upper wall (UW). The regions with a pressure difference are connected by porous of the UW and by the air cavity AC. Therefore, the air is transfered through the AC in a direction from the high-pressure region +P to the low-pressure region -P. Thus, the pressure difference between the two regions is redistributed and is reduced. For this reason the propeller noise is decreased.

Thus, 'butterfly acoustical skin' will become a very effective means to improve acoustic performances of the propeller-based propulsion systems. A higher acoustical performance of propeller blades with BAS can improve flying quality, safety, and comfort of passengers and residents of airport neighborhood. It can reduce detectability in military operations (detection of an aircraft with this propeller by an enemy's passive acoustic system can be difficult). In addition to the aircraft, the butterfly skin could also be used in jet engines and in submarines.

Acknowledgments

The author would like to thank my advisor Dr. Olga Bocharova–Messner for her comments. The author thanks the external reviewers for their constructive comments. The author would like to acknowledge the Zaporozhye Machine-Building Design Bureau for its collaboration.

References

[1] Leishman, J. G. Principles of Helicopter Aerodynamics (Cambridge aerospace series). 2006, p. 817.

[2] Hubbard, H. H. Aeroacoustics of Flight Vehicles: Theory and Practice. NASA. 1991, 1, p. 610.

[3] Holmes, J. B.; Durham, H. M. and Tarry, E. S. Small Aircraft Transportation System Concept and Technologies. Journal of Aircraft. 2004, 41 (1), 26 – 35.

[4] Smith, S. W. The Scientist and Engineer's Guide to Digital Signal Processing. (California Technical Publishing). 1997, p. 643.

[5] Theodorsen, T. and Regler, A. A. The Problem of Noise Reduction with Reference to Light Airplanes. NACA 1145, 1946.

[6] Metzger, F. B. An Assessment of Propeller Aircraft Noise Reduction. Technology NASA. 1995, 198237.

[7]Mixson, J.; Greene, G. and Dempsey, T. Sources, Control and Effects of Noise From Aircraft Propellers and Rotors. NASA. 1981, 81971.

[8] Hoehne, V. O. and Luce, R. G. The Quieted Aircraft as a Military Tool. AIAA. 1969, Paper 792.

[9] Fulghum, A. D. Stealth Now. Aviation Week and Space Technology. 2005, 162, 13, p. 38.

[10] Sobieszczanski-Sobieski, J. and Haftka, R. T. Multidisciplinary Aerospace Design Optimization: Survey of Recent Developments. Structural Optimization. 1997, 14, 1 – 23.

[11] Benyus, J. M. Biomimicry: Innovation Inspired by Nature (New York: William Morrow); 1997; p. 320.

[12] Capinera, John L. Encyclopedia of Entomology. Butterflies and moths. 4, 2nd ed.: Springer, 2008; pp. 626–672.

[13]Brown. The book of butterflies, sphinxes and moths; illustrated by one hundred and forty-four engravings, coloured after nature; in three volumes, 1832.

[14] Kovalev, I. S. Effect of the scales coverage of the moth gastropacha populifolia esper (*Lepidoptera*, *lasiocampidae*) on the reflection of the bat echolocation signal. Entomological Review. 2004, 83, 513 – 515.

[15] Ntelezos, A.; Guarato, F. and Windmill, J. F. C. The anti-bat strategy of ultrasound absorption: the wings of nocturnal moths (Bombycoidea: Saturniidae) absorb more ultrasound than the wings of diurnal moths (Chalcosiinae: Zygaenoidea: Zygaenidae), Biology Open. 2017, 6, 109 – 117.

[16] Jinyao Zeng, Ning Xiang, Lei Jiang, Gareth Jones, Yongmei Zheng, Bingwan Liu, Shuyi Zhang. Moth Wing Scales Slightly Increase the Absorbance of Bat Echolocation Calls. PloS One. 6 : e27190.

[17] Zhiyuan Shen, Thomas R. Neil, Daniel Robert, Bruce W. Drinkwater, and Marc W. Holderied. Biomechanics of a moth scale at ultrasonic frequencies. Proceedings of the natural Academy of Sciences. 2018, 115:48, 12200-12205.

[18] Kovalev, I. S. Acoustic properties of wing scaling in Noctuid Moth. Entomological Review. 2003, 82 (2), 270 – 275.

[19] Kovalev, I. S. and Brodsky, A. K. Of the role that elasticity and scales coating of the wings play in the flight stability of insects. Bulletin of the S. Petersburg State University. 1996, 3 (3), 3-7.

[20] Hooijdonk, E.; Vandenbem, C.; Berthier, S. and Vigneron, J. Bi-functional photonic structure in the (Papilionidae): modeling by scattering-matrix optical simulations. Opt. Express. 2012, 20, 22001 – 22011.

[21] Trzeciak, T. M.; Wilts, B. D.; Stavenga, D. G. and Vukusic, P. Variable multilayer reflection together with long-pass filtering pigment determines the wing coloration of papilionid butterflies of the nireusgroup. Opt. Express. 2012, 20, 8877 - 8890.

[22] Stavenga, D. G.; Stowe, S.; Siebke, K.; Zeil, J. & Arikawa, K. Butterfly wing colours: scale beads make white pierid wings brighter. Proc. R. Soc. B. 2004, 271, 1577–1584.

[23]Roger, M. and Moreau, S. Broadband self-noise from loaded fan blades. AIAA Journal. 2004, 42(3), 536–544.

[24] Pagano, M.; Barbarino, D.; Casalino, P. and Federico, L. Tonal and Broadband Noise Calculations for Aeroacoustic Optimization of Propeller Blades in a Pusher Configuration. Journal of Aircraft. 2010, 47(3).

[25] Sinibaldi, G. and Marino, L. Experimental analysis on the noise of propellers for small UAV. Applied Acoustics. 2013, 74, 79 – 88.

[26] Pechan, T. and Sescu, A. Experimental study of noise emitted by propeller's surface imperfections. Applied Acoustics. 2015, 92, 12 – 17.

[27] Hamakawa, H.; Hosokai, K.; Adachi, T.; Kurihara, E. Aerodynamic Sound radiated from Two-Dimensional Airfoil with Local Porous Material. Open Journal of Fluid Dynamics. 2013, 3, 55 – 60.

[28] Flumerfelt, J. F. Aluminum powder metallurgy processing. Retrospective Theses and Dissertations. 1998, 11918.

[29] Sarradj, E. and Geyer, T. Noise generation by porous airfoils. 13th AIAA/CEAS aeroacoustics conference. 2007, 3719.

[30] Rackl, G.; Miller, G.; Guo, Y. and Yamamoto, K. Airframe Noise Studies - Review and Future Direction. NASA. 2005, 213767.

[31] Lee, S. Effect of leading-edge porosity on blade-vortex interaction noise. AIAA. 1993, 0601.

[32] Magliozzi, B.; Hanson, D. B. and Amiet, R. K. Propeller and Propfan Noise. NASA . 1991, 1258.

[33] Allard, J. F. Propagation of Sound in Porous Media: Modelling Sound Absorbing Materials. John Wiley & Sons. 2009, p. 351.

[34] Crocker, M. J. and Arenas, J. P. Use of Sound-Absorbing Materials. John Wiley and Sons. 2007, 696-713.

[35] Tinetti, A.; Kelly, J.; Thomas, R. and Bauer, S. Reduction of Wake-Stator Interaction Noise Using Passive Porosity. 40th AIAA Aerospace Sciences Meeting and Exhibit. 2002, 1036.